Manuscript Information

Journal name: Current biology : CB

NIHMSID: NIHMS228168

Manuscript Title: Novel role for Netrins in regulating epithelial behavior during lung branching morphogenesis.

Principal Investigator:

Submitter: William J. Brunken (william.brunken@downstate.edu)

Grant/Project/Contract/Support Information

Name	Support ID#	Title
William J. Brunken	R01 NS039502-04	STRUCTURE AND FUNCTION OF NON BASEMENT MEMBRANE LAMININS

Manuscript Files

Type	Fig/Table #	Filename	Size	Uploaded
manuscript		Liu et al - 04 (Hogan).pdf	5193009	2010-08-11 15:32:48

This PDF receipt will only be used as the basis for generating PubMed Central (PMC) documents. PMC documents will be made available for review after conversion (approx. 2-3 weeks time). Any corrections that need to be made will be done at that time. No materials will be released to PMC without the approval of an author. Only the PMC documents will appear on PubMed Central -- this PDF Receipt will not appear on PubMed Central.

Novel Role for Netrins
in Regulating Epithelial Behavior
during Lung Branching Morphogenesis

Yuru Liu,[1,6] Elke Stein,[2] Timothy Oliver,[1] Yong Li,[3]
William J. Brunken,[3] Manuel Koch,[4]
Marc Tessier-Lavigne,[5] and Brigid L.M. Hogan[1,*]
[1]Department of Cell Biology
Duke University Medical Center
Durham, North Carolina 27710
[2]Department of Molecular, Cellular
   and Developmental Biology
Yale University
New Haven, Connecticut 06510
[3]Department of Anatomy and Cellular Biology
Tufts University School of Medicine
Boston, Massachusetts 02111
[4]Institute for Biochemistry II
University of Köln
50931 Köln
Germany
[5]Genetech, Inc.
1 DNA Way
South San Francisco, California 94080

Summary

The development of many organs, including the lung, depends upon a process known as branching morphogenesis, in which a simple epithelial bud gives rise to a complex tree-like system of tubes specialized for the transport of gas or fluids. Previous studies on lung development have highlighted a role for fibroblast growth factors (FGFs), made by the mesodermal cells, in promoting the proliferation, budding, and chemotaxis of the epithelial endoderm [1–3]. Here, by using a three-dimensional culture system, we provide evidence for a novel role for Netrins, best known as axonal guidance molecules [4, 5], in modulating the morphogenetic response of lung endoderm to exogenous FGFs. This effect involves inhibition of localized changes in cell shape and phosphorylation of the intracellular mitogen-activated protein kinase(s) (ERK1/2, for extracellular signal-regulated kinase-1 and -2), elicited by exogenous FGFs. The temporal and spatial expression of netrin 1, netrin 4, and Unc5b genes and the localization of Netrin-4 protein in vivo suggest a model in which Netrins in the basal lamina locally modulate and fine-tune the outgrowth and shape of emergent epithelial buds.

Results and Discussion

The branching morphogenesis of the mouse lung starts at embryonic day (E)9.5 (E9.5), when two primordial buds composed of an inner endodermal epithelium and an outer mesenchymal jacket appear in the ventral-lateral wall of the foregut. Between E9.5 and E16.5 (the pseudo-

*Correspondence: b.hogan@cellbio.duke.edu
[6]Present address: Ben May Institute for Cancer Research, University of Chicago, Chicago, IL 60637.

glandular stage), the primordial buds give rise to the respiratory tree [1–3]. This process requires FGFR2IIIb, a receptor isoform expressed in the endoderm, and FGFs made in the mesoderm. Expression of *Fgf10* is highly localized to the distal mesoderm adjacent to the tips of developing buds, while *Fgf7* is expressed more diffusely and at lower levels early in lung development [6]. Recent studies suggest that extracellular factors, such as heparan sulfate proteoglycans, locally modulate FGF activity [7]. However, the role of other extracellular molecules, such as Netrins, in lung branching morphogenesis has not been explored.

In mammals, there are three netrin genes, *netrin 1*, *netrin 3*, and *netrin 4*, two genes encoding related proteins (Netrin-G1 and -G2), and two conserved families of transmembrane receptors. DCC (deleted in colorectal cancer) receptors are responsible for mediating the attraction response of axons to Netrins, while UNC5 family members, either as homodimers or heterodimers with DCC proteins, mediate repulsion [4, 5, 8–10]. Until recently, functional analysis of Netrins and their receptors has focused on the nervous system, but evidence is emerging for in vivo roles in other organ systems, including the mammary gland and inner ear [11, 12]. Additionally, in vitro assays have suggested a role for Netrin in the adhesion and migration of pancreatic epithelial cells [13].

Previous studies on the embryonic lung localized Netrin-1 protein to proximal epithelial cells and underlying smooth muscle [14], but netrin gene expression was not examined. We therefore compared the patterns of expression of *netrin 1*, *netrin 3*, and *netrin 4* during lung development by using in situ hybridization. As shown in Figure 1, *netrin 1* and *netrin 4* have very similar transcription domains; RNA levels are highest in the nonbranching proximal endoderm and in the stalk or neck region of the flask-shaped distal buds but are excluded from the dilated region at the tips. Once the major events of branching morphogenesis cease, *netrin 1* expression decreases dramatically (Figure 1G). In contrast to the other netrin genes, *netrin 3* is transcribed throughout the endoderm and mesoderm (Figures 1H and S1D [in the Supplemental Data available with this paper online]). Among the classical Netrin receptors, DCC is localized at E11.5 to the basal-lateral membrane of proximal endoderm and to the apical surface of distal epithelium (Figures 1K and 1L). *Neogenin* and *Unc5c* (*rcm*) are expressed exclusively in the mesoderm at E13.5 (Figure S1, Supplemental Data). No transcripts for *Unc5a* and *Unc5d* could be detected in either the mesoderm or endoderm, but *Unc5b* is clearly transcribed in both these cell populations in the distal lung (Figures 1M and 1N and data not shown). Thus, both DCC and *Unc5b* are expressed in lung epithelial cells and available to transduce Netrin signals during branching morphogenesis.

As mentioned above, Netrin-1 protein was localized to the epithelial cells and underlying smooth muscle of embryonic mouse lung [14]. To localize Netrin-4 protein, we carried out immunohistochemistry with E13.5 lung
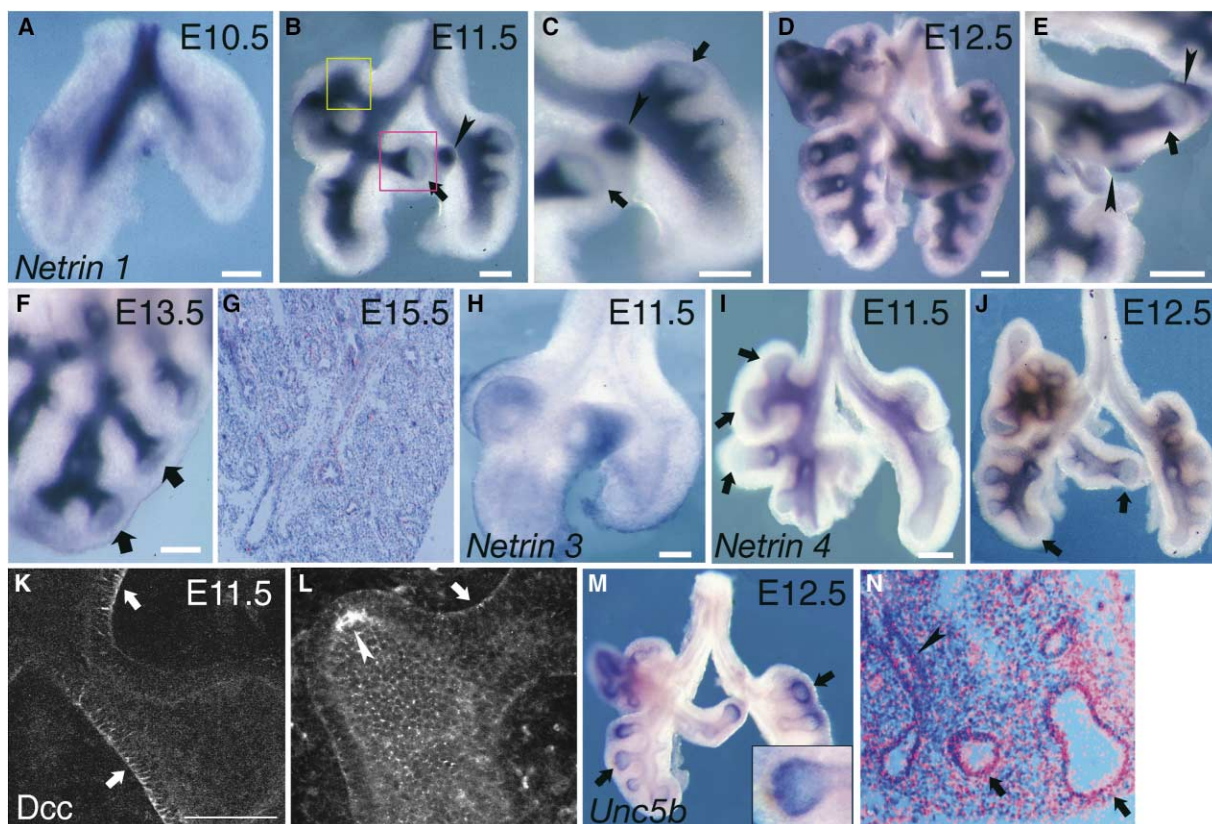
Figure 1. Spatial and Temporal Expression of Genes Encoding Netrins and Their Receptors during Lung Branching Morphogenesis

(A)–(F), (H)–(J), and (M) are the results of whole mount and (G and N) radioactive section in situ hybridization. *netrin 1* is expressed at E10.5 (A), continues at E11.5 (B and C), E12.5 (D and E), and E13.5 (F) but dramatically declines by E15.5 (G). Transcripts are present in the proximal epithelium and enriched in the stalks of buds but are excluded from the dilated distal tips (arrows in [B], [C], and [E]). (C) and (E) are enlargements of (B) and (D), respectively. Discrete regions of distal mesoderm in the right accessory and medial lobes also show *netrin 1* expression (arrowheads in [B], [C], and [E]). (H) *netrin 3* is expressed diffusely at low levels throughout the lung endoderm and mesoderm at E11.5. *netrin 4* is expressed in proximal, but not distal, endoderm (arrows) at E11.5 (I) and E12.5 (J). (K and L) At E11.5, whole-mount immunohistochemistry localized DCC basally in the proximal endoderm (arrows) and apically in distal epithelium at the tips of buds (arrowhead in [L]). (K) and (L) correspond to the approximate positions of the pink and yellow squares in (B). (M and N) *Unc5b* transcripts are present in distal endoderm (arrows) and mesenchyme, but not in proximal endoderm (arrowhead) at E12.5 (M) and E13.5 (N). Inset in (M) shows that *Unc5b* is expressed in distal tip and neck region of endoderm. Scale bar = 100 μm.

by using two different affinity-purfied antisera. Since both gave similar results, only one is shown in Figure 2. Netrin-4 is deposited in the basement membrane of the proximal endoderm and stalk regions, where it colocalizes with perlecan but is absent from around the distal tips of the buds. Together with the in situ hybridization results, these data suggest that Netrin-4 is produced by the endoderm and is incorporated into the subjacent basal lamina. There is no evidence for localization of the protein in the surrounding mesenchyme.

To study the response of lung epithelium to Netrins, we used an in vitro culture system in which mesenchyme-free distal epithelium is cultured in Matrigel in serum-free medium with FGF7 [6, 7, 15]. Within several hours of being placed in culture, the epithelium forms a vesicle with the apical cell surfaces facing the inner lumen (Figures 3 and S2A and Movie 1). After about 48 hr, control samples incubated with 30 ng/ml FGF7 show numerous secondary buds on the surface (Figure 3A). Paradoxically, higher concentrations of FGF7 (e.g., 1 μg/ml) have a different effect, in that few or no buds

are seen (Figure S3A and see reference [7]). Strikingly, when 10–50 μg/ml recombinant mouse or human Netrin-4 is added to the Matrigel with the lower concentrations of FGF7, all the samples examined at 48 hr have a smooth surface with no secondary buds (Figure 3B). Significantly, the same effect is achieved by using a truncated form of Netrin-4 lacking the C domain (N4delC, Figure 3C). This domain may mediate dimerization of Netrin-4 [9]; in Netrin-1, the C domain appears to mediate binding to matrix and integrins [13]. A similar suppression of budding is seen with recombinant chicken and mouse Netrin-1 (Figure 3D). However, a higher concentration (50 μg/ml) is needed to achieve this inhibition compared with Netrin-4. The effect of added Netrin is better understood when followed by time-lapse microscopy. In control samples, secondary buds first appear on the surface of the endoderm at around 20 hr and extend to an average length of about 60 μm over the next 24 hr (Figures 3G–3L). By contrast, if 50 μg/ml exogenous Netrin-4 is added, clusters of cells form localized "knobs" projecting into the lumen of the cyst rather than buds ex-
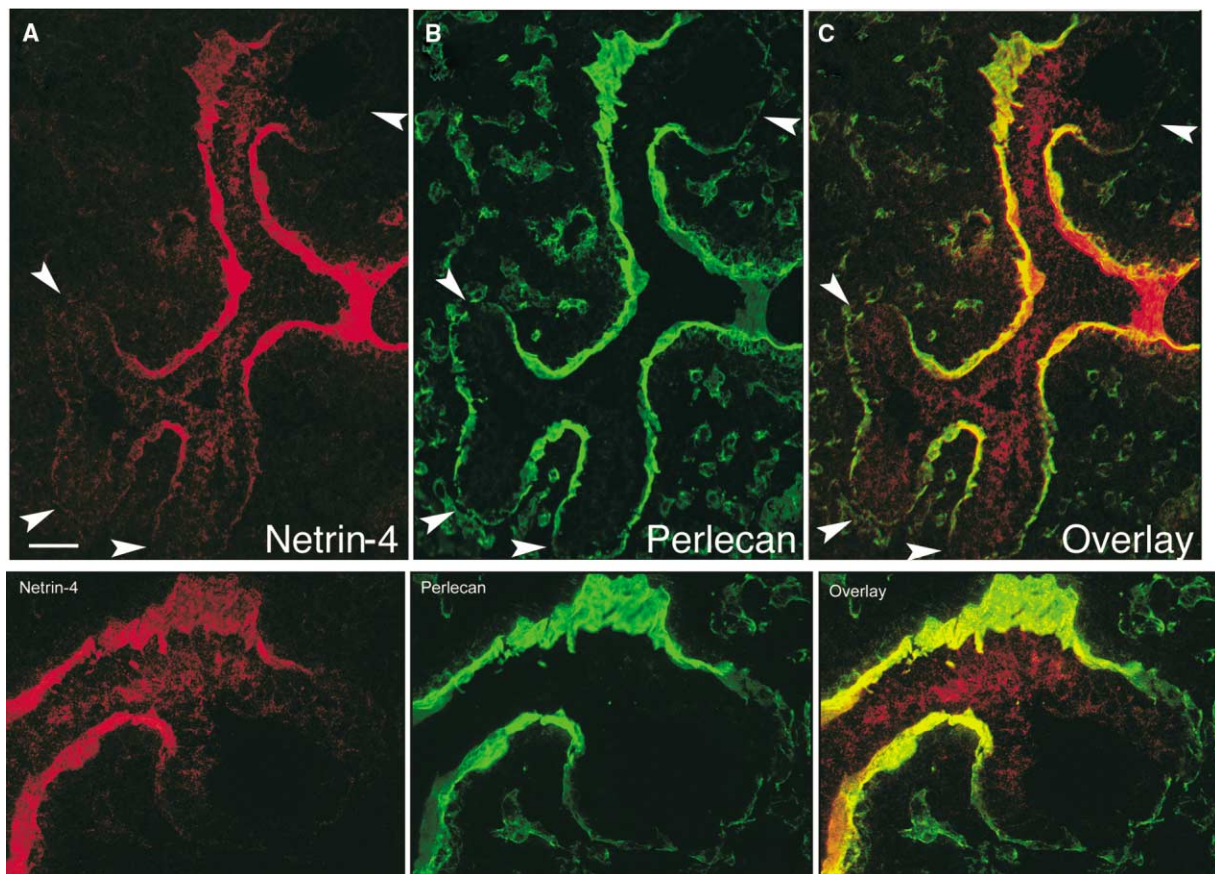
Figure 2. Netrin-4 Is Expressed in the Basement Membrane of Proximal, but Not Distal, Lung Endoderm

Sections of E13.5 mouse lung were incubated with Netrin-4 and Perlecan primary antibodies. Digital images were then deconvolved. They demonstrate that Netrin-4 ([A], red) is colocalized to the basement membrane with Perlecan ([B], green) in the proximal region of the developing airway (yellow to orange in [C], overlay). In the distal bud regions (arrowheads), Netrin-4 protein is absent, while Perlecan is present. This is shown more clearly in the higher power images of the top right terminal bud in the bottom panels. Scale bar is 40 μm for upper panels and 20 μm for lower panels.

tending from the surface (Figures 3M–3R and see Movie 1). These knobs later mostly disappear as the cells become incorporated into the epithelium of the cyst. Analysis of the internalized cells by confocal microscopy shows that most of them retain their epithelial phenotype and express the junctional protein ZO-1 on the surface facing the lumen (see Figure S2).

Previous studies in 3D (Matrigel) culture have shown that the response of lung endoderm to 30–1000 ng/ml FGF10 is different from that to FGF7; fewer buds are formed and they are thinner and longer (on average about 100 μm long after 48 hr [15]. As shown in Figures S3C and S3D, 50 μg/ml exogenous Netrin-4 significantly reduces the number of elongated buds in the presence of FGF10.

Experiments were carried out to test the specificity and mechanism of action of exogenous Netrin-4 (or 50 μg/ml exogenous Netrin-1) on endoderm cultured under standard conditions in Matrigel with 30 ng/ml FGF7. First, the effect is reversible; if samples treated with Netrin for 40 hr are reembedded in fresh Matrigel with FGF7 alone, numerous buds subsequently appear on the surface (Figures 3S–3V). Second, the effect of Netrin

is not mimicked by adding either 50-200 μg/ml soluble mouse Laminin or 50 μg/ml recombinant mouse Netrin-G1a, neither of which is thought to bind to DCC and UNC5 [10] (Figures 3E and 3F). Immunohistochemical assays using antibody to phosphorylated Histone H3 to monitor cell proliferation and antibody to cleaved Caspase-3 to stain apoptotic cells both failed to show any significant differences between control and Netrin-treated samples (Figures 4A–4C and data not shown). The conclusion that Netrin is not functioning in this system as a mitogen or survival factor is further strengthened by the following observation. Endoderm in 3D Matrigel cultures containing exogenous Netrin cannot survive without FGFs, nor do endoderm cultures appear healthier than control cultures when 5 ng/ml FGF7, which is the minimum concentration for survival, is present in the medium (data not shown). Other experiments have determined that four marker genes—*Pea3*, *surfactant protein C (Sftpc)*, *Bmp4*, and *Sox9*—are preferentially active in distal, compared with proximal, lung endoderm. Moreover, they are upregulated in vitro by added FGF7 [15, 16]. Expression of these markers was not changed by exogenous Netrins, even when the budding
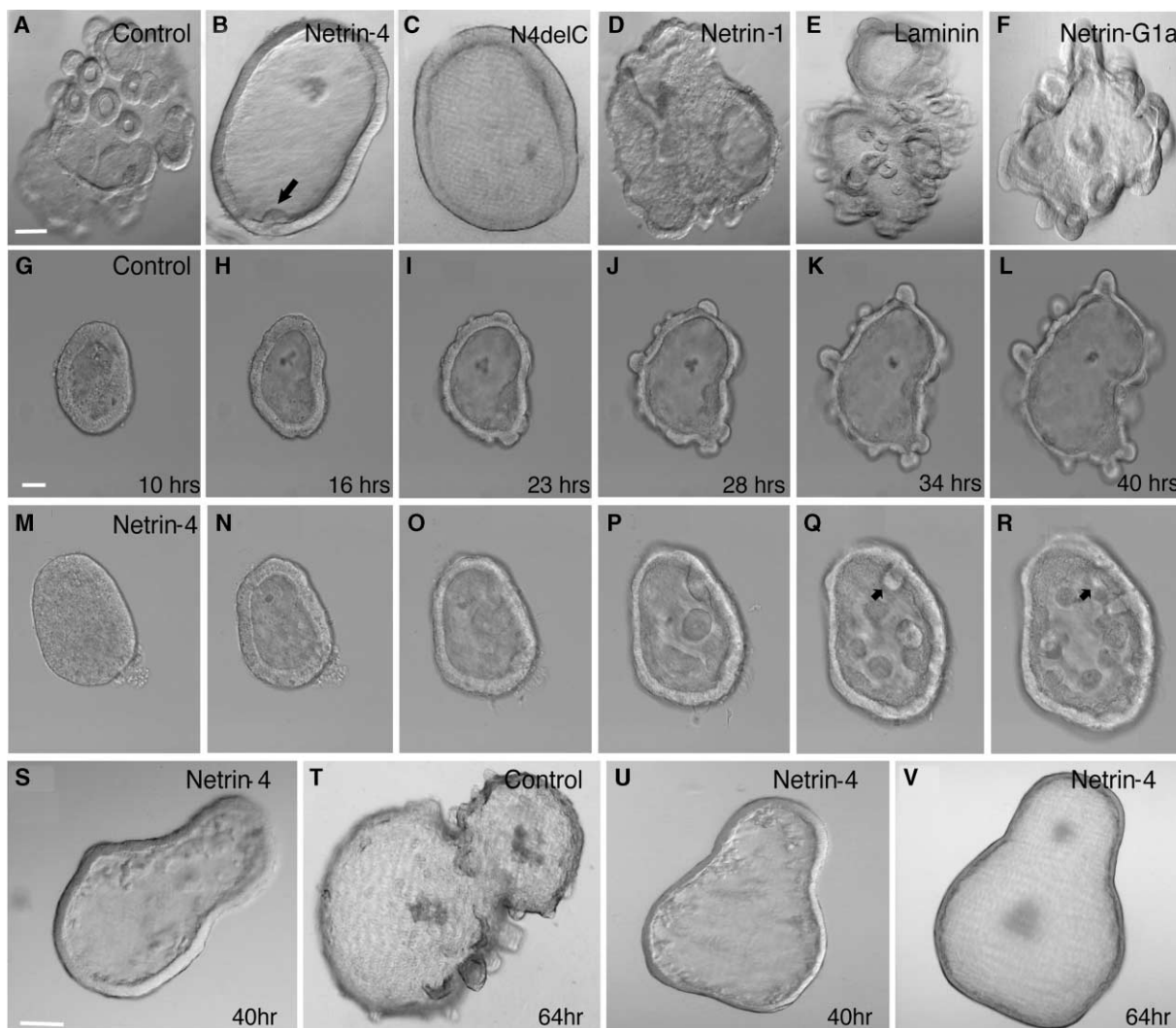
Figure 3. Morphological Response of Cultured Endodermal Epithelium to Exogenous FGF7 and Netrins

(A–F) DIC images of isolated endoderm after 40 hr culture in control Matrigel (A) or Matrigel containing 50 μg/ml full-length Netrin-4 (B), C-terminal truncated N4delC (C), Netrin-1 (D), Laminin (E), or Netrin-G1a (F). Note the presence of numerous secondary buds in (A), (E), and (F) but not in (B), (C), and (D). Arrow in (B) indicates a knob of cells inside the cyst. (G–R) Selected time-lapse images of endoderm cultured without (G–L) or with 50 μg/ml Netrin-4 (M–R). For the complete sequence see Movies in the Supplemental Data. Note the numerous secondary buds that form at the surface of control samples, while knobs of cells form inside of cyst in samples cultured with Netrin-4. As growth proceeds, the internal cells are incorporated into the surface epithelium (arrows in [Q] and [R]). (S–V) The morphological changes induced by Netrin-4 are reversible. After 40 hr culture in the presence of Netrin-4 (S and U), the endoderm is transferred to new Matrigel with FGF7, but without netrin. 24 hr later, numerous secondary buds formed in control gel (T), but not in gel containing Netrin-4 (V). All cultures are supplemented with 30 ng/ml FGF7. Scale bar = 100 μm.

response was strongly inhibited (see Figure S4). *Unc5b* continues to be expressed in the epithelium of Netrin-treated samples even though the normal sites of highest gene expression, the secondary buds, are absent (Figure 4). Finally, functional blocking antibody to DCC (AF5; 5 μg/ml) did not block the budding in response to FGF7 or the inhibition of budding by added Netrin (see Figure S5). These observations suggest that the response to exogenous Netrin is mediated by Unc5b rather than by DCC, although a role for integrins [13] cannot be excluded.

With effects on cell proliferation, survival, and differentiation ruled out, the most likely mechanism by which exogenous Netrins could act is by inhibiting the changes in cell shape and/or MAP kinase activity associated with bud initiation. Studies in other systems have demonstrated that phosphorylation of intracellular ERK1/2 is associated with changes in actin binding proteins and cell adhesion molecules and is required for branching morphogenesis of uretic buds [17, 18]. We therefore used confocal microscopy to correlate cell morphology and MAP kinase activity in lung buds in vivo and in vitro. In vitro, endoderm cells in nonbudding areas are organized into either cuboidal or pseudostratified layers and have a centrally located nucleus (Figures 4H and 4I). By contrast, cells at the tips of FGF7-induced buds are
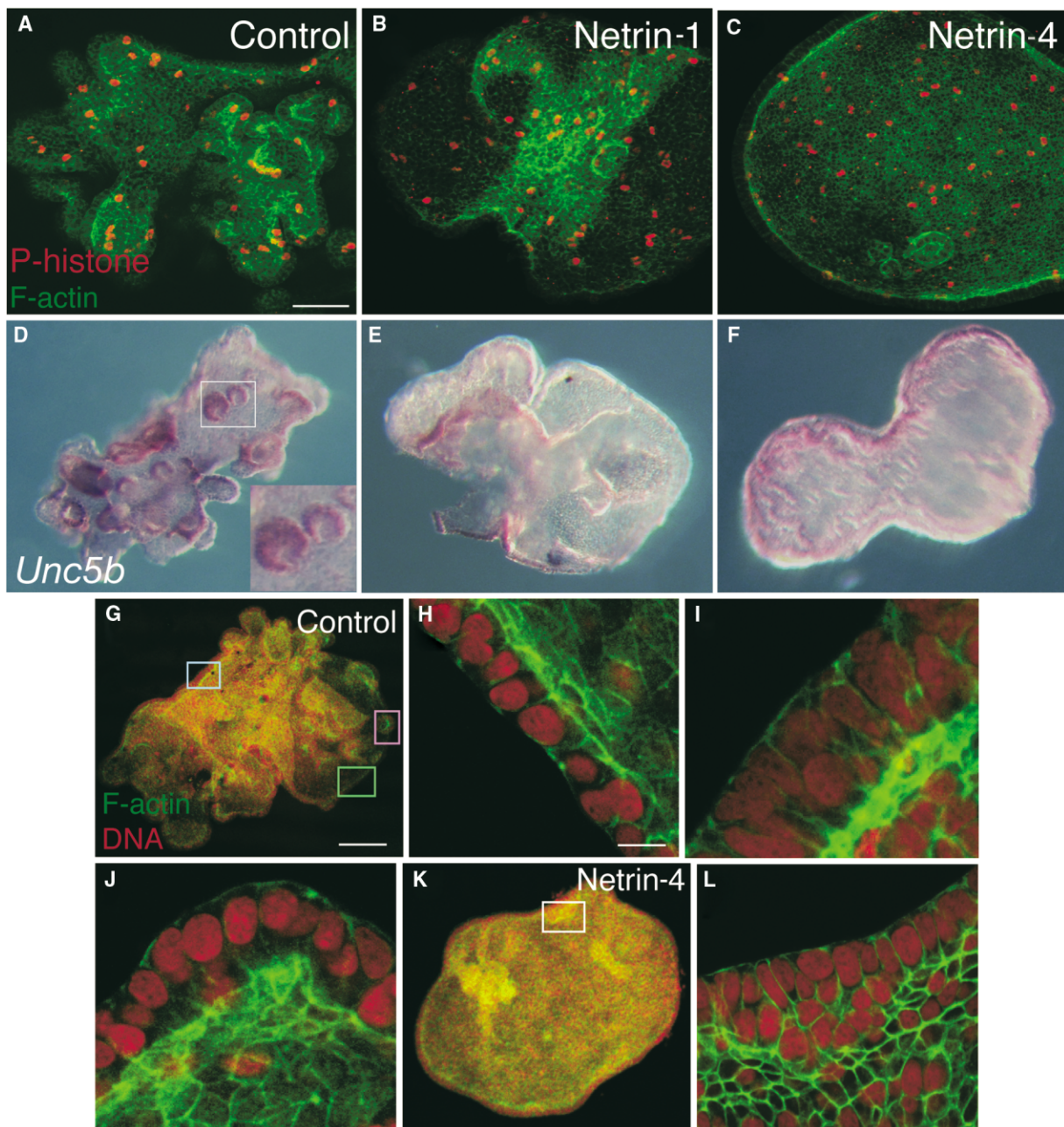
Figure 4. Cell Proliferation, *Unc5b* Expression, and Cell Shape Change after Exogenous Netrin Treatment

(A–C) Cell proliferation in control (A) and Netrin-1-treated endoderm (B) or Netrin-4-treated (C) endoderm is estimated by double labeling with antibody to phospho-Histone H3 (red), and Alexa Fluor 488 phalloidin (green), which labels filamentous actin.

(D–F) Expression of *Unc5b* in control (D) and Netrin-1-treated (E) or Netrin-4-treated (F) endoderm examined by whole-mount in situ hybridization. Inset in (D) shows elevated expression in secondary buds.

(G–L) Cell shape visualized by double labeling with Alexa Fluor 488 phalloidin (green) and propidium iodide (red). (G–J) In control endoderm, epithelial cells in nonbudding areas are arranged in either a cuboidal ([H], corresponding to approximately the green square in [G]) or pseudostratified layer ([I], blue square in [G]). (J) In the secondary bud (pink square in [G]), cells have an elongated wedge shape and basally localized nuclei. (K and L) In Netrin-4-treated samples, cells in the internal knobs have an irregular shape (L). Scale bar = 100 μm for (A–G) and (K), 10 μm for other panels.

wedge shaped, with their nuclei located basally (Figure 4J). Immunohistochemistry reveals that these cells contain significantly higher levels of phosphoERK1/2 than cells in the interbud zones relative to total ERK1/2 proteins, which are evenly distributed (Figures 5A, 5D, and 5F). By contrast, phosphoAkt, another downstream target of FGF, does not appear to be differentially distributed between bud and interbud zones (data not shown). The localization of higher phosphoERK1/2 activity in the tips of the buds is particularly clear in samples grown in
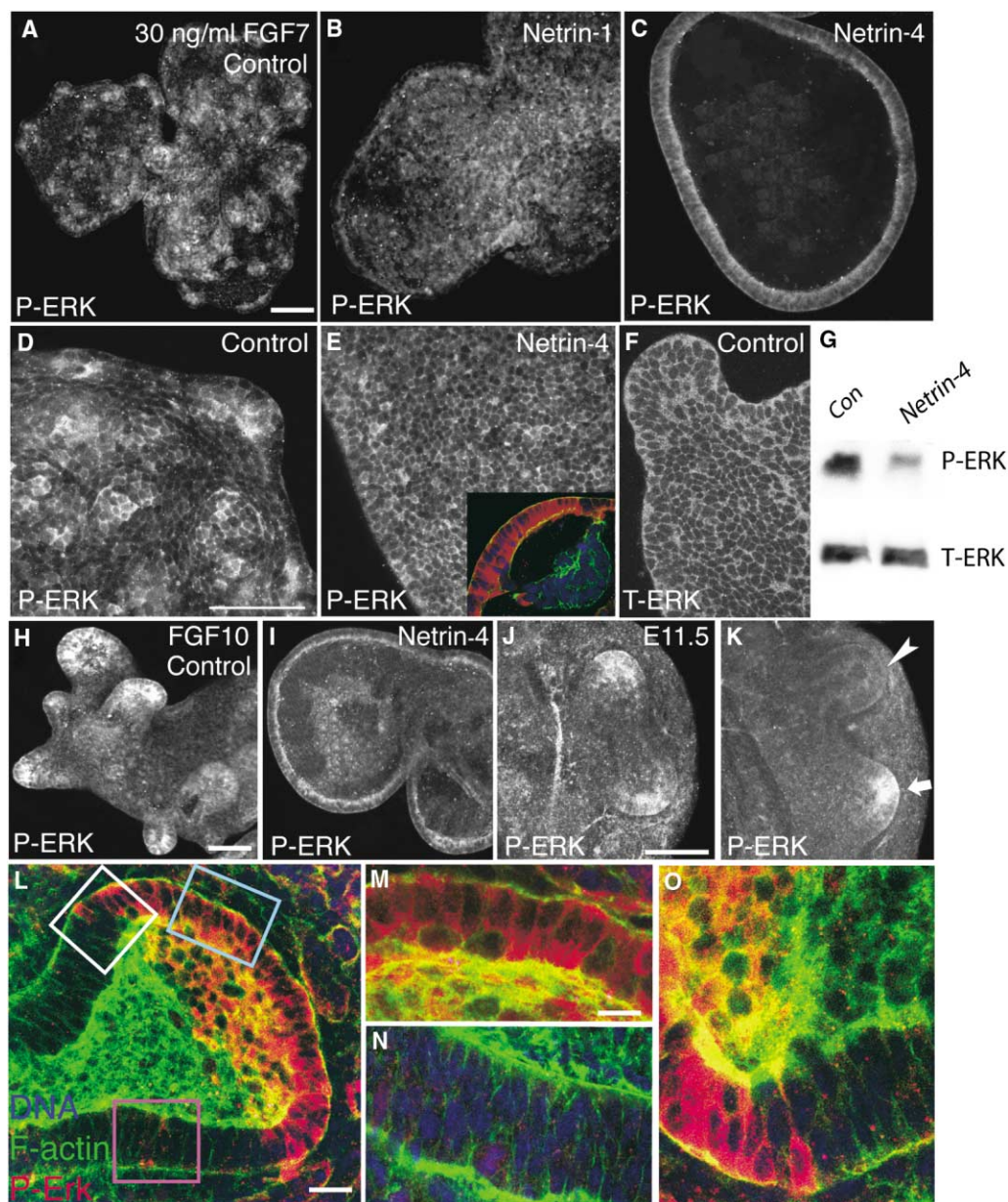
Figure 5. Distribution of PhosphoERK1/2 in Control and Netrin-Treated Endoderm and E11.5 Lung

ERK1/2 activity is assayed by whole mount immunohistochemistry by using antibody specific for phosphorylated forms of the protein. (A–E) endoderm cultured in Matrigel and 30 ng/ml FGF7 either without (A and D) or with 50 μg/ml Netrin-1 (B) or Netrin-4 (C and E). Note the elevated levels of phosphoERK1/2 in the secondary buds (A and D) but more uniform distribution in Netrin-treated samples (B, C, and E). The focal plane is through the lumen of the cysts in (C) and (I) and near the surface for (A, B, D–F, and H). Inset in (E) shows absence of phosphoERK1/2 in the internalized knobs in Netrin-4-treated samples. (F) Total ERK1/2 is distributed uniformly among budding and interbudding zone. (G) Western blot analysis shows that the relative level of phosphoERK1/2 is decreased in Netrin-4-treated samples. (H and I) In control samples cultured with 250 ng/ml FGF10, localized phosphoERK1/2 is restricted to the tips of elongated secondary buds (H), while Netrin-4-treated endoderm shows a uniform, low level of phosphoERK1/2 activity (I). (J–O) PhosphoERK1/2 activity in normal E11.5 lung. Note that highest ERK1/2 activity is localized to the distal tip of endodermal buds, and initiating buds shows higher phosphoERK than elongating buds (compare arrow and arrowhead in [K]). (L–O) When labeled together with TOTO-3 (blue, to visualize nuclei) and Alexa Fluor 488 phalloidin (green), a sharp boundary is seen between epithelial cells in the dilated distal tip of buds, which show high ERK1/2 activity (red), and the stalk region showing low levels. (M), (N), and (O) correspond to the blue, pink, and white squares in (L), respectively. Scale bar = 100 μm for (A)–(I), 20 μm for (J)–(L), and 10 μm for (M)–(O).

the presence of FGF10 (Figure 5H). A similar correlation between phosphoERK activity and epithelial cell morphology is also detected in vivo, for example, in the tips of newly formed lateral buds in the E11.5 lung. Confocal microscopy reveals a sharp boundary between the mostly wedge-shaped cells with strong phosphoERK staining in the distal tip of the bud and the predominantly pseudostratisfied epithelial cells in the "neck" of the

flask-shaped bud, which have much lower activity (Figures 5J–5O). Interestingly, analysis of endoderm samples cultured in Matrigel with high concentrations of FGF7 (1 μg/ml) show a uniform distribution of strong phosphoERK staining throughout the epithelium, even though buds do not form (see Figures S3A, S3E, and S3F). This raises the possibility that a differential distribution of phosphoERK protein between cells in the tips and stalks is required for bud morphogenesis and outgrowth.

Two indirect lines of evidence support a role for FGF/MAP kinase pathway activity in lung epithelial budding morphogenesis. First, transfection of a bronchial epithelial cell line in vitro with a plasmid encoding activated Ras promotes a significant change in cell shape so that cells are more spread and have prominent lamellipodia (Figures S6A and S6B). Second, the inhibitor U0126, which blocks MEK1 (MAP kinase kinase) activity, inhibits budding in response to FGF7 (Figures S6C and S6D).

Confocal microscopy of endoderm samples cultured in Matrigel with both Netrin and 30 ng/ml FGF7 shows that nearly all the cells have centrally located nuclei, and localized peaks of very strong MAP kinase activity are absent. Rather, the level of phosphoERK1/2 is relatively uniform throughout the epithelium (Figures 5B, 5C, and 5E). Moreover, internal cells lack phosphoERK1/2 staining. Western blotting of extracts of treated and control endoderm samples confirms the overall lower level of phosphorylated ERK seen in Netrin-treated samples by immunohistochemistry (Figure 5G). These results suggest a model in which Netrin inhibits bud morphogenesis in vitro by acting through its receptor(s) in the endoderm to block the formation of local peaks of phosphoERK1/2 activities that normally drive bud initiation and/or outgrowth.

Taken together with the localization of Netrin RNA and protein during lung development, these in vitro results suggest the following model for the role of Netrins during early branching morphogenesis. A bud is initiated in response to a localized concentration of FGF10 in the mesoderm, probably stabilized by extracellular sulfated proteoglycans, which activate ERK1/2 as part of the downstream signaling cascade. In response to the differential distribution of MAP kinase activity, buds elongate and move away from the original stem. Netrin-1 and -4, secreted by the epithelial cells in the proximal lung and base and necks of buds, are deposited locally in the basal lamina underlying the cells. Here, they act, possibly through Unc5b, to inhibit ERK kinase and thus prevent ectopic budding and fine-tune the size and shape of emerging buds (Figure 6A). In support of this hypothesis, activation of Unc5b during axonal guidance decreases ERK1/2 activity (E.S., unpublished data). However, at this time we cannot rule out the involvement of other receptor(s).

One prediction of this model is that early branching morphogenesis should be abnormal in lungs lacking genes encoding Netrins or Netrin receptors. We therefore examined lungs of embryos homozygous for a strong hypomorphic allele of *netrin 1* and a null allele of *netrin 4*. However, at E11.5–E13.5 no significant difference in lung morphology was seen between any genotypes. Similarly, $Dcc^{-/-}$ mutants showed no obvious
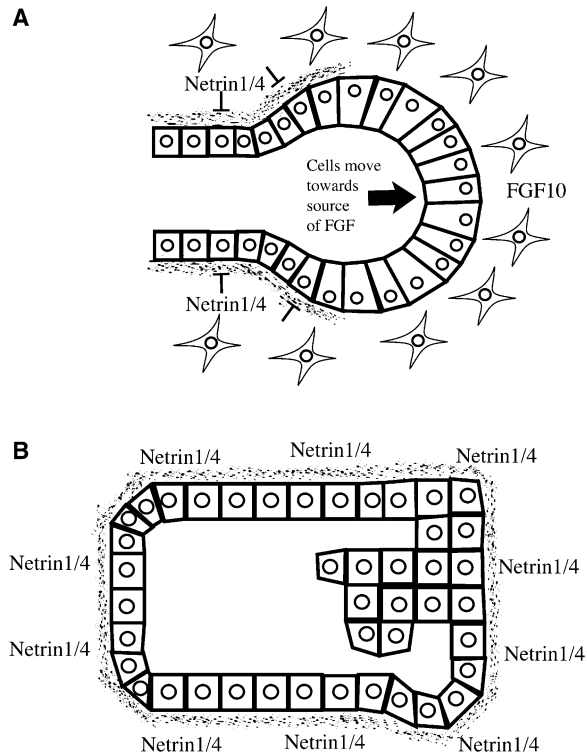

Figure 6. A Model for the Possible Roles Played by Netrins during Lung Epithelial Branching Morphogenesis

(A) Netrin-1 and -4 made by epithelial cells are deposited at the basement membrane and/or bind locally to epithelial cells at the neck region of elongating endoderm buds. Here they act through Unc5b or an unknown receptor to decrease the local ERK1/2 activity in the endoderm, thus facilitating the outgrowth of buds toward the source of FGF10 in the mesoderm, as well as preventing the generation of ectopic buds. According to this model, the basal lamina plus Netrins acts as a kind of sleeve or "corset," restricting the morphogenesis of the emerging bud.

(B) Our in vitro assays in which endoderm is surrounded by basal lamina components in the Matrigel mimic the effect of localized, ectopic Netrins at the distal tip, thus preventing bud outgrowth. In contrast, some cells accumulate at the inside of the lumen and form internal knobs.

phenotype at the same stage. These results suggest that there is a high degree of functional redundancy among the various Netrins and receptors. Deletion of multiple netrin genes, possibly on a sensitized mutant background such as heterozygosity for *Fgf10* or in combination with mutations in genes encoding other guidance molecules such as Slit2 [27, 28], will be required for the manifestation of a branching phenotype. These possibilities are under investigation.

Experimental Procedures

Mouse Strains and Breeding
Lungs were dissected from ICR mice at E11.5 (noon on the day of plug is E0.5) and processed for in situ hybridization, immunohistochemistry, or in vitro culture as described [19]. The *Bmp4-lacZ* reporter mouse line has been described [19].

Mice heterozygous for *netrin 1*($Ntn\ 1^{Gt(pGT1.8TM)629Ecs}$), *netrin 4*, and *Dcc* were maintained by interbreeding. Genotyping of the *netrin 1* and *Dcc* locus was performed as described [20, 21]. PCR primers 5′-AGCAGCCTTTAAACATCCTGAG-3′ and 5′-CAAATGTGTCAGTT

TCATAGCC-3′ were used for the genotyping of the *netrin 4* locus. For *netrin 1*[-/-] lungs, 4, 12, and 4 examples were examined at E11.5, E12.5, and E13.5, respectively. For *netrin 4*[-/-] lungs, 4 and 5 samples were examined at E11.5 and E12.5, respectively. For *Dcc*^{-/-} lungs, 4 and 6 examples were examined at E12.5 and E13.5, respectively.

In Situ Hybridization

Whole-mount in situ hybridization was performed by using digoxygenin-labeled antisense RNA probes as described [15]. The probes for *netrin 1*, *netrin 3*, *Unc5a*, *Unc5b*, *Unc5d*, and *neogenin* have been described [20–24]. The *netrin 4* [25] and *Unc5c* [24] probes were kindly provided by Dr. Joshua R. Sanes and Dr. Susan Ackerman, respectively. At least three samples were examined for each probe.

Radioactive section in situ hybridization was performed as described by using S[35]-labeled RNA probes [6].

Lung Endoderm Culture

Mesenchyme-free distal lung endoderm was isolated as described and cultured in Matrigel in serum-free medium consisting of Ham's F12:DMEM 50:50, 1% BSA, and 2 mM glutamine [15]. The medium was supplemented with FGF7 (R&D Systems) or FGF10 (kindly provided by Dr. N. Itoh, Kyoto University) at the concentrations indicated. In some experiments, 50 μg/ml recombinant chicken or mouse Netrin-1, mouse or human Netrin-4, mouse Netrin G1a (R&D Systems), or Laminin (Sigma) was mixed with the Matrigel. The abilities of full-length rNetrin-1 and rNetrin-4 to bind Unc5b have been assayed by the manufacturer. rN4delC, a truncated Netrin-4 lacking the C domain was mixed in both the Matrigel and medium at 50 μg/ml. Mouse monoclonal antibodies against DCC (AF5, Oncogene) were included at 5 μg/ml, in both the Matrigel and the culture medium. The MEK inhibitor, U0126 (Promega), was used at 10 μM. Following incubation at 37°C and 5% CO_2/95% air for 40 hr, the endoderm was released from Matrigel by matrisperse treatment (BD Bioscience) [15] and processed for in situ hybridization or antibody staining. Each culture condition was repeated at least three times with about ten endoderm samples per experiment.

The time-lapse movies were made on a fully motorized Zeiss Axiovert 200 equipped with "cell observer" environmental control system (featuring independent control of specimen temperature, microscope temperature, specimen CO2%, and humidity). DIC images were repeatedly collected at indicated times under lowest possible lighting levels, consistent with obtaining a good-quality digital image at the expense of 2 × 2 pixel binning and elevated camera gain. Metamorph v6.1 (Universal Imaging. Inc.) was used to acquire and edit images through the multidimensional acquisition/review dialogs, and 12 bit raw tiff format images were exported into Quicktime and AVI movies.

Immunohistochemistry, Immunoblotting, and Staining
for β-Galactosidase Activity

Whole-mount antibody staining was carried out as previously described [19]. The following antibodies were used at the given concentrations: rabbit anti-mouse Sox9 (a kind gift from Dr. Francis Poulat at CNRS, Montpellier) (0.5 μg/ml); mouse anti-DCC AF5 (Oncogene) (5 μg/ml); rabbit anti-phospho-Histone H3 (Upstate Technology) and cleaved Caspase-3 (Cell Signaling) (1:500 and 1:50, respectively); rabbit anti-ZO-1 (Zymed) (2.5 μg/ml); rabbit anti-Sftpc (Chemicon) (1:500); rabbit polyclonal antibody against phosphorylated p44/42 ERK (Cell Signaling) (1:350) [26]; and rabbit polyclonal antibody against total p44/42 ERK (Cell Signaling) (1:100). Two preparations of rabbit polyclonal Netrin-4 antibodies were used: R33 and KR1, R33 was characterized and published [9], and KR1 was raised against the same antigen. Both have no reactivity in the *netrin 4* null mutant mouse (W.J.B., Y.L, and M.K., unpublished data). Lung sections from E13.5 mouse were prepared and stained for Netrin-4 as described [9]. To reconstruct Netrin-4 protein in lung, a Z axis stack of images was taken by using conventional microscopic images at 0.25 μm steps, which were deconvolved by using the three nearest neighbor algorithm (OpenLab 3,5.1; Improvision LTD, Lexington, MA).

In some experiments, the tissues were also labeled with 0.13 μM Alexa Fluor 488 phalloidin or 25 nM TOTO-3 (Molecular Probes), or

0.3 μg/ml propidium iodide (Sigma) and the images collected by using Zeiss LSM 510 confocal microscopy.

Immunoblotting was performed by using endoderm samples grown with 300 ng/ml FGF7 in control Matrigel and Matrigel mixed with 50 μg/ml rNetrin-4. Protein extracts of 30 endoderm samples were loaded on each lane and antibodies to total ERK (Sigma) and PhosphoERK (Cell signaling) were used at 1:10,000 and 1:500, respectively. This experiment was repeated three times.

Staining for β-galactosidase activity was performed as described [15].

Transfection of Bronchial Epithelial Cells
with Activated Ras

The human bronchial epithelial cell line 16HBE14o- was cultured as described [29]. The cells were transfected either with MIGR1-RasL61, which expresses an activated form of Ras [30], or vector control by using TransIt-LT-1 transfection reagent (Mirus). The morphology of the cells was examined after 36 hr, and the cells expressing the transfected gene were identified by a GFP marker that is coexpressed via an IRES site in the vector. The 16HBE14o- cells and MIGR1-RasL61 construct were kindly provided by Drs. Mark Abe and Akira Imamoto (University of Chicago), respectively.

Supplemental Data

Supplemental Data including five figures and two movies are available at http://www.current-biology.com/cgi/content/full/14/10/897/DC1/.

References

1. Hogan, B.L. (1999). Morphogenesis. Cell *96*, 225–233.
2. Warburton, D., Schwarz, M., Tefft, D., Flores-Delgado, G., Anderson, K.D., and Cardoso, W.V. (2000). The molecular basis of lung morphogenesis. Mech. Dev. *92*, 55–81.
3. Cardoso, W. (2001). Molecular regulation of lung development. Annu. Rev. Physiol. *63*, 471–494.
4. Tessier-Lavigne, M., and Goodman, C. (1996). The molecular biology of axon guidance. Science *274*, 1123–1133.
5. Yu, T., and Bargmann, C. (2001). Dynamic regulation of axon guidance. Nat. Neurosci. Suppl. *4*, 1169–1176.
6. Bellusci, S., Grindley, J., Emoto, H., Itoh, N., and Hogan, B.L. (1997). Fibroblast growth factor 10 (FGF10) and branching morphogenesis in the embryonic mouse lung. Development *124*, 4867–4878.
7. Izvolsky, K., Shoykhet, D., Yang, Y., Yu, Q., Nugent, M., and Cardoso, W. (2003). Heparan sulfate-FGF10 interactions during lung morphogenesis. Dev. Biol. *258*, 185–200.
8. Puschel, A. (1999). Divergent properties of mouse netrins. Mech. Dev. *83*, 65–75.
9. Koch, M., Murrell, J.R., Hunter, D.D., Olson, P.F., Jin, W., Keene, D.R., Brunken, W.J., and Burgeson, R.E. (2000). A novel member of the netrin family, beta-netrin, shares homology with the beta chain of laminin: identification, expression, and functional characterization. J. Cell Biol. *151*, 221–234.
10. Nakashiba, T., Nishimura, S., Ikeda, T., and Itohara, S. (2002). Complementary expression and neurite outgrowth activity of netrin-G subfamily members. Mech. Dev. *111*, 47–60.

11. Salminen, M., Meyer, B., Bober, E., and Gruss, P. (2000). Netrin 1 is required for semicircular canal formation in the mouse inner ear. Development *127*, 13–22.

12. Srinivasan, K., Strickland, P., Valdes, A., Shin, G., and Hinck, L. (2003). Netrin-1/neogenin interaction stabilizes multipotent progenitor cap cells during mammary gland morphogenesis. Dev. Cell *4*, 371–382.

13. Yebra, M., Montgomery, A., Diaferia, G., Kaido, T., Silletti, S., Perez, B., Just, M., Hildbrand, S., Hurford, R., Florkiewicz, E., et al. (2003). Recognition of the neural chemoattractant Netrin-1 by integrins alpha6beta4 and alpha3beta1 regulates epithelial cell adhesion and migration. Dev. Cell *5*, 695–707.

14. Dalvin, S., Anselmo, M., Prodhan, P., Komatsuzaki, K., Schnitzer, J., and Kinane, T. (2003). Expression of Netrin-1 and its two receptors DCC and UNC5H2 in the developing mouse lung. Gene Expr. Patterns *3*, 279–283.

15. Liu, Y., Jiang, H., Crawford, H.C., and Hogan, B. (2003). Role for ETS domain transcription factors Pea3/Erm in mouse lung development. Dev. Biol. *261*, 10–24.

16. Liu, Y., and Hogan, B.L. (2002). Differential gene expression in the distal tip endoderm of the embryonic mouse lung. Mech Dev. Gene Expr. Patterns *2*, 229–233.

17. Fisher, C., Michael, L., Barnett, M., and Davies, J. (2001). Erk MAP kinase regulates branching morphogenesis in the developing mouse kidney. Development *128*, 4329–4338.

18. Ishibe, S., Joly, D., Zhu, X., and Cantley, L. (2003). Phosphorylation-dependent paxillin-ERK association mediates hepatocyte growth factor-stimulated epithelial morphogenesis. Mol. Cell *12*, 1275–1285.

19. Weaver, M., Dunn, N.R., and Hogan, B.L. (2000). Bmp4 and Fgf10 play opposing roles during lung bud morphogenesis. Development *127*, 2695–2704.

20. Serafini, T., Colamarino, S., Leonardo, E., Wang, H., Beddington, R., Skarnes, W., and Tessier-Lavigne, M. (1996). Netrin-1 is required for commissural axon guidance in the developing vertebrate nervous system. Cell *87*, 1001–1014.

21. Keino-Masu, K., Masu, M., Hinck, L., Leonardo, E., Chan, S., Culotti, J., and Tessier-Lavigne, M. (1996). Deleted in Colorectal Cancer (DCC) encodes a netrin receptor. Cell *87*, 175–185.

22. Leonardo, E., Hinck, L., Masu, M., Keino-Masu, K., Ackerman, S., and Tessier-Lavigne, M. (1997). Vertebrate homologues of C. elegans UNC-5 are candidate netrin receptors. Nature *386*, 833–838.

23. Wang, H., Copel, N., Gilbert, D., Jenkins, N., and Tessier-Lavigne, M. (1999). Netrin-3, a mouse homolog of human NTN2L, is highly expressed in sensory ganglia and shows differential binding to netrin receptors. J. Neurosci. *19*, 4938–4947.

24. Engelkamp, D. (2002). Cloning of three mouse Unc5 genes and their expression patterns at mid-gestation. Mech. Dev. *118*, 191–197.

25. Yin, Y., Sanes, J., and Miner, J. (2000). Identification and expression of mouse netrin-4. Mech. Dev. *96*, 115–119.

26. Corson, L., Yamanaka, Y., Lai, K., and Rossant, J. (2003). Spatial and temporal patterns of ERK signaling during mouse embryogenesis. Development *130*, 4527–4537.

27. Brose, K., Bland, K.S., Wang, K.H., Arnott, D., Henzel, W., Goodman, C.S., Tessier-lavigne, M., and Kidd, T. (1999). Slit proteins bind Robo receptors and have an evolutionarily conserved role in repulsive axon guidance. Cell *96*, 795–806.

28. Anselmo, M.A., Dalvin, S., Prodhan, P., Komatsuzaki, K., Aidlen, J.T., Schnitzer, J.J., Wu, J.Y., and Kinane, T.B. (2003). Slit and Robo: expression patterns in lung development. Gene Expr. Patterns *3*, 13–19.

29. Cozens, A.L., Yezzi, M.J., Kunzelmann, K., Ohrui, T., Chin, L., Eng, K., Finkbeiner, W.E., Widdicombe, J.H., and Gruenert, D.C. (1994). CFTR expression and chloride secretion in polarized immortal human bronchial epithelial cells. Am. J. Respir. Cell Mol. Biol. *10*, 38–47.

30. Minden, A., Lin, A., McMahon, M., Lange-Carter, C., Derijard, B., Davis, R.J., Johnson, G.L., and Karin, M. (1994). Differential activation of ERK and JNK mitogen-activated protein kinases by Raf-1 and MEKK. Science *266*, 1719–1723.

Supplemental Data

Novel Role for Netrins in Regulating Epithelial Behavior during Lung Branching Morphogenesis

Yuru Liu, Elke Stein, Timothy Oliver, Yong Li, William J. Brunken, Manuel Koch, Marc Tessier-Lavigne, and Brigid L.M. Hogan
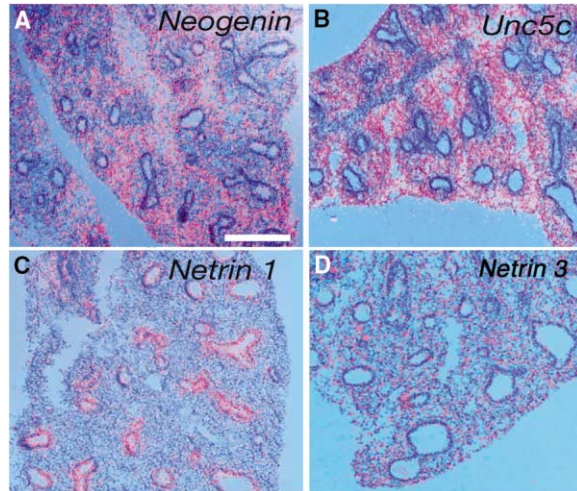
Figure S1. Expression of Genes Encoding Netrin and Receptors in Embryonic Lungs

Section in situ hybridizations show that at E13.5, *neogenin* (A), and *Unc5c* (B) are expressed predominantly in the mesoderm, while *netrin 1* (C) is expressed exclusively in the endoderm and *netrin 3* (D) is expressed at low levels in endoderm and mesoderm. Scale bar = 100 μm.
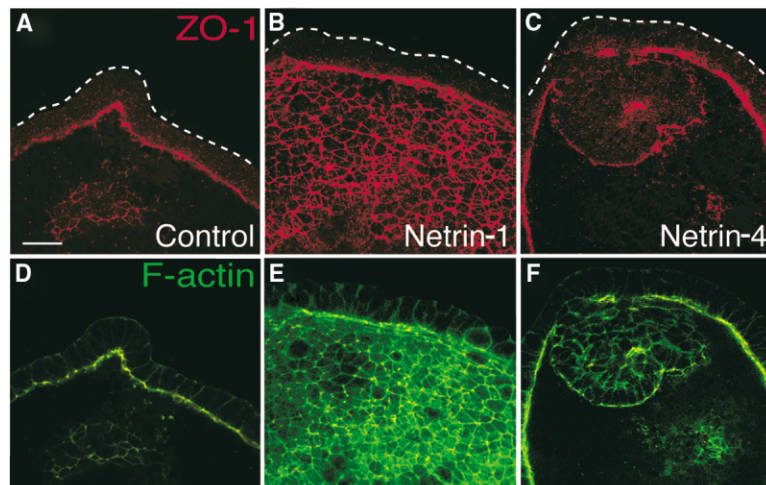
Figure S2. Epithelial Cell Polarity in Control and Netrin-Treated Endoderm

(A–C) Whole-mount antibody staining with the apical marker ZO-1 followed by confocal microscopy shows that the apical side of the epithelium is facing the lumen in control (A) as well as Netrin-1-treated (B) and Netrin-4-treated (C) endoderm cultures. Note some of the internalized cells in Netrin-4-treated cells lose ZO-1 staining. Dotted line shows outline of the basal surface of epithelium.

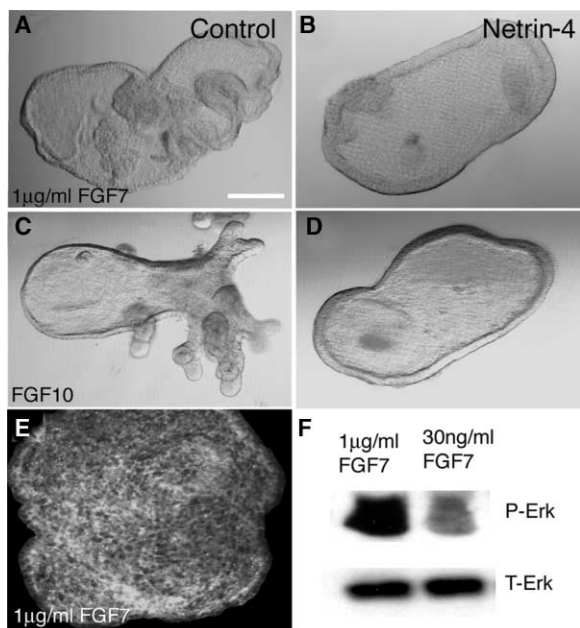(D–F) Double labeling with Alexa Fluor 488 phalloidin to visualize the outline of the cells. Scale bar = 100 μm.

Figure S3. Morphological Response of Cultured Endoderm toward
1 μg/ml FGF7, FGF10, and Netrin-4

(A and B) When the medium is supplemented with very high concen-
trations of FGF7 (1 μg/ml), both control and Netrin-4-treated endo-
derm form cysts with a smooth surface and few secondary buds.
Internalized groups of cells were frequently observed in control
samples, as well as with Netrin.

(C and D) When grown with 50–1000 ng/ml FGF10, the endoderm
forms elongated buds in control gel (on average 6.16 buds per
sample, n = 34) but form a significantly reduced number of buds
in the presence of Netrin-4 (on average 0.3 buds per sample,
n = 50).

(E and F) When endoderm is grown with 1 μg/ml FGF7, the distribu-
tion of phosphoERK1/2 is relatively uniform (E). The level of phos-
phoERK1/2 is higher in endoderm grown in 1 μg/ml FGF7 than the
buds grown with 30 ng/ml FGF7, while the amount of total ERK1/2
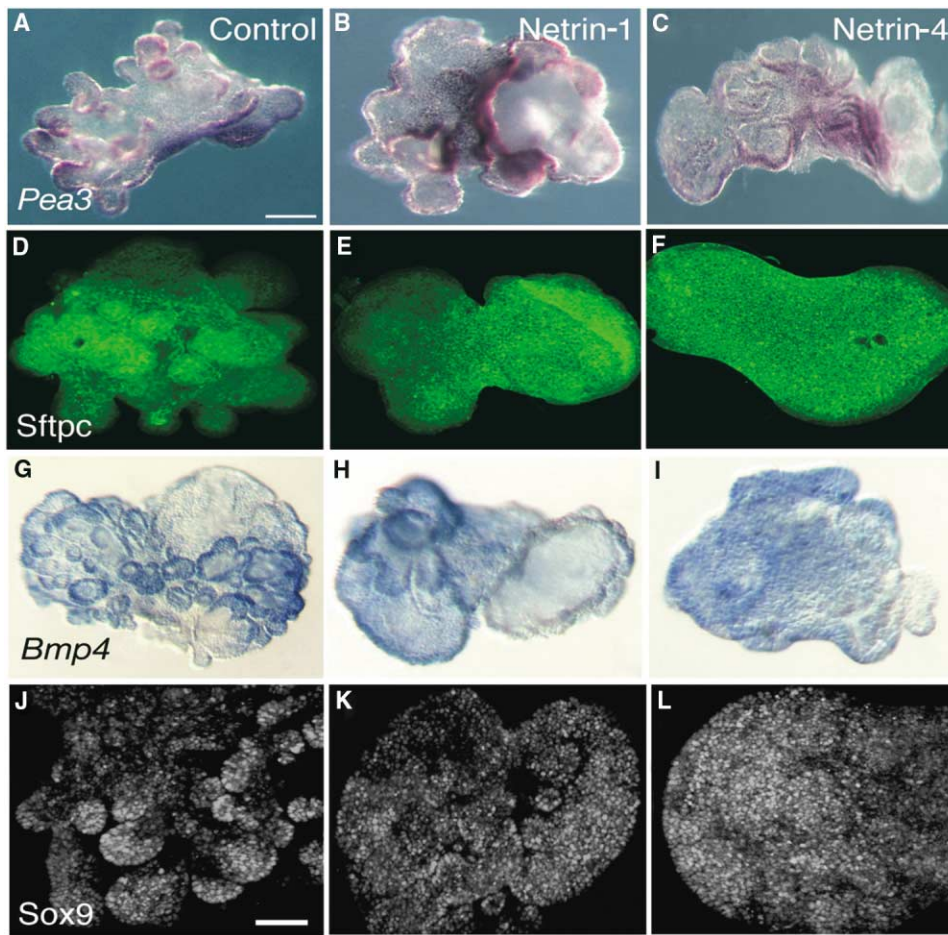is the same (F). Scale bar = 100 μm.

Figure S4. Expression of Distal-Specific Genes after Netrin Treatment

Expression of distal-specific genes *Pea3* (A–C), Sftpc (D–F), *Bmp4-lacZ* (G–I), and Sox9 (J–L) in control (A, D, G, and J) and Netrin-1-treated (B, E, H, and K) or Netrin-4-treated (C, F, I, and L) endoderm. (A)–(C) show whole-mount in situ hybridization with an antisense *Pea3* RNA probe, while (D–F) and (J–L) show whole-mount immunohistochemistry with an antibody against Sftpc or Sox9. A *Bmp4-lacZ* reporter line was used to visualize the expression of *Bmp4* (G–I). Scale bar = 100 μm.
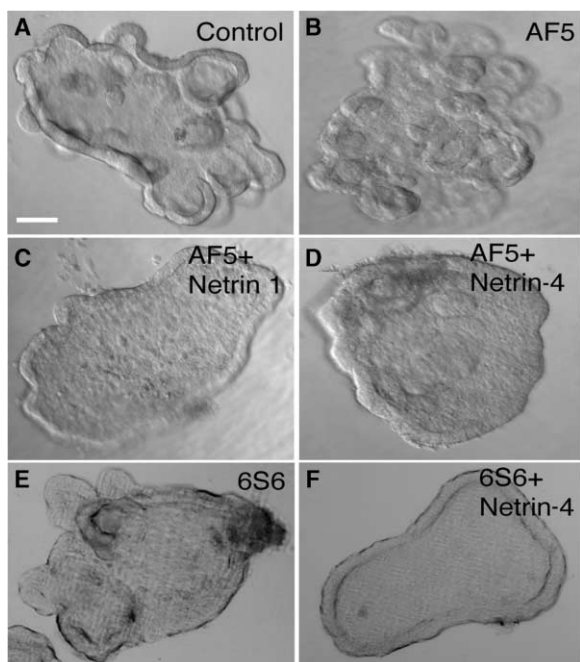
Figure S5. The Effect of DCC Blocking Antibody, AF5

(A–D) When 5 μg/ml AF5 is present in the culture medium, the endoderm cyst is less expanded (B) than in control samples (A) but still forms secondary buds. When 50 μg/ml Netrin-1 (C) or 20 μg/ml Netrin-4 (D) is mixed in the Matrigel, the endoderm cysts fail to form secondary buds in the presence of AF5.
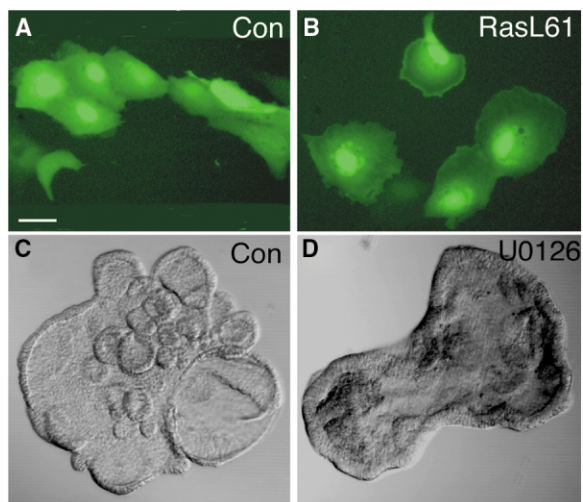

Figure S6. Evidence that the FGF/MAP Kinase Signaling Pathway Regulates Lung Epithelial Cell Morphogenesis

(A and B) Transfection of a human bronchial epithelial cell line with DNA encoding an activated form of Ras (H-RasL61) (B) changes cell morphology compared with vector control (A).

(C and D) 10 μM U0126, a MEK inhibitor, inhibits the formation of secondary buds in the presence of 30 ng/ml FGF7. Scale bar = 6μm for (A) and (B) and 60μm for (C) and (D).